

TRACING MATTER WITH WEAK LENSING SURVEYS

Y. MELLIER^{1,2}, L. van WAERBEKE^{1,3}

¹*IAP, 98 bis boulevard Arago; 75014 Paris, France.*

²*Observatoire de Paris, DEMIRM 61 avenue de l'Observatoire; 75014 Paris, France.*

³*CITA, Mc Lennan Labs., 60 St George Street; Toronto, Ont. M5S 3H8 Canada.*

Abstract. Gravitational weak lensing maps the location of (dark) matter at all scales. The lens-induced distortion field traces gravity fields and can be used to reconstruct the mass distribution in galaxies, groups, clusters of galaxies or large-scale structures. From these reconstructions, one can in principle recover where the matter is, what are its properties and how it is coupled with light and baryons. In the following, we review the present status of weak lensing analysis and discuss the most recent results regarding matter properties in the universe.

1 Introduction

Gravitational lensing by foreground structures induces image deformation of all distant galaxies. Spectacular cases caused by infinite magnification eventually produce giant arcs and multiple images configuration, but these are exceptional events: in general the amplitude of the distortion is weak and can be detected only statistically over a large number of galaxies. In this 'weak lensing' regime, a non-parametric mass reconstruction provides projected mass maps of the Universe.

The distortion field is given by a line-of-sight projection of the mass density contrast. This distortion field is measured from the shape of the lensed galaxies which is characterized by the surface brightness second moments $I(\boldsymbol{\theta})$, (see [1], [2] and references therein):

$$M_{ij} = \frac{\int I(\boldsymbol{\theta}) \theta_i \theta_j d^2\theta}{\int I(\boldsymbol{\theta}) d^2\theta} . \quad (1)$$

A galaxy with intrinsic ellipticity \mathbf{e} is then measured with an ellipticity $\mathbf{e} + \boldsymbol{\delta}$, where $\boldsymbol{\delta}$ is the distortion of the galaxies, given by

$$\boldsymbol{\delta} = 2\gamma \frac{(1 - \kappa)}{(1 - \kappa)^2 + |\gamma|^2} = \left(\delta_1 : \frac{M_{11} - M_{22}}{Tr(M)} ; \delta_2 : \frac{2M_{12}}{Tr(M)} \right) . \quad (2)$$

κ and γ are respectively the gravitational convergence and shear, which both depend on the second derivative of the projected gravitational potential, φ :

$$\kappa(\boldsymbol{\theta}) = \frac{1}{2} (\varphi_{,11} + \varphi_{,22}); \quad \gamma_1(\boldsymbol{\theta}) = \frac{1}{2} (\varphi_{,11} - \varphi_{,22}); \quad \gamma_2(\boldsymbol{\theta}) = \varphi_{,12} = \varphi_{,21} . \quad (3)$$

Equations (2) and (3) characterize the relation between the projected mass density and the ellipticity of lensed galaxies. Hence, they provide a recipe to recover the projected gravity field from the distortion field. In the case of weak lensing, the galaxy ellipticity is a direct measure of the shear ($\kappa \ll 1$ and $|\gamma| \ll 1$, and therefore $\delta \approx 2\gamma$) which makes the mass reconstruction a simple linear operation.

During the past decade, spectacular theoretical and technical developments in weak lensing analyses lead to the production of a new mass estimator which in principle works at all scales. Weak lensing reconstruction has been mostly used on galaxies, clusters of galaxies and large-scale structures. The scientific outcomes coming from these different analysis are presented and discussed in this review.

2 Properties of galaxy halos

Diagnostics about the properties of galaxy halos are important tests of CDM scenarios. According to the numerical simulations of cosmic structures, galaxies are very dense systems with a cuspy mass

profile and mass density slopes similar to NFW family. These predictions can be tested with galaxy-galaxy lensing or mass reconstruction using weak distortion maps or strong lensing statistics.

The galaxy-galaxy lensing analysis consists in separating a foreground population of galaxies (*ie* the lenses) from a background sample (*ie* the lensed galaxies). An averaged distortion is then measured around all the foreground galaxies. The investigation of galaxy halos is done by comparing the expected distortion field, inferred from analytical mass profiles, to the observed one, computed from ellipticities of background galaxies. The properties of analytical profiles are characterized by a velocity dispersion or circular velocity, a physical scale, and a slope.

The orientation φ of the background galaxies with respect to the line joining the galaxy and the foreground lens is given by ([3]):

$$p(\varphi) = \frac{2}{\pi} \left[1 - \gamma_t \left\langle \frac{1}{\epsilon^s} \right\rangle \cos(2\varphi) \right]. \quad (4)$$

Which means that the lensed galaxies are preferentially tangentially aligned with the lens ($\varphi \simeq 90$). ϵ^s is the ellipticity of the (unlensed) background galaxy and γ_t is the tangential component of the gravitational shear. In practice, we have to take into account the fact that mass profiles of nearby foreground galaxies overlap (Schneider & Rix 1997; [4]), but it does not change the general principle of the technique which was pioneered by Tyson et al (1984: [5]).

Quantitative results regarding the properties of galaxy halos have been first obtained by Brainerd et al ([3]) and are still in progress using big imaging surveys (see [1], [2]). The most recent ones use jointly imaging and spectroscopic data in order to scale the amount of lensing mass and the total luminosity of galaxies from the redshift distribution of foreground and background galaxies. McKay et al 2001 ([6]) and Smith et al 2000 ([7]) used respectively the SDSS and the LCRS survey and obtained detailed galaxy-galaxy analysis. Both agree with earlier works that typical velocity dispersion or circular velocity of lensing galaxies range between 120 to 220 km/sec. The radial distribution of the shear is compatible with a power law close to an isothermal profile, but there is not yet conclusive evidence they are better fit than NFW profile. Likewise, the typical physical scale is still uncertain and ranges between 20 to 250 h^{-1} kpc. The upper limit seems compatible with the most recent analyses and implies that the contribution of galaxy halos to Ω_m could be very large, possibly $0.1 < \Omega_{gal} < 0.25$. Wilson et al. (2001; [8]) adopted a different strategy to analyze early type galaxy halos of their survey (they compared a projected luminosity map with a mass map from weak lensing reconstruction) and they reached similar conclusions regarding Ω_{gal} .

The cuspy nature of galaxy halo is hard to test using weak lensing analysis since it cannot scales smaller than 100 pc. However, such small scales are accessible with strong lensing statistics which measures the frequency of events like multiple images of lensed quasars. For instance, highly peaked mass density profiles produces a central image strongly demagnified, not visible in practice. This lensing property of cuspy profiles is an important difference from soft core mass models and this was exploited by Keeton (2001; [9]) to explore the inner profile of the lenses in the CLASS sample of radio galaxies. It turns out that only few lenses do have visible odd image, whereas about 30% of the sample should show one, according to theoretical expectations from CDM models. If Keeton's interpretation is correct, galaxies are more cuspy than CDM halos. Surprisingly, the fraction of gravitational lenses of the CLASS sample lead to an opposite conclusion on scale larger than 10 kpc: CDM halos are too concentrated compared to galaxies. This paradox is somewhat confusing but is a very interesting diagnostic regarding the description of dark galaxy halos and its interpretation in the context of galaxy formation processes at very small scale.

Within the class of models he studied, Keeton addressed many issues and concluded that his results are robust, and the associated uncertainties well understood. Nevertheless, it is not yet obvious that his conclusions can be compared with galaxy-galaxy lensing because the scales probed in the later are much larger. Moreover, it must be keep in mind that Keeton's star+halo model may be only a partial description of galaxies. On the other hand, if the size of halos are as large as 250 h^{-1} kpc, then galaxy-galaxy lensing parameters may be significantly contaminated by other foreground galaxies or by additional effects produced by groups or clusters of galaxies.

3 Clusters of galaxies

Gravitational growth of structure formation predicts that clusters of galaxies are dynamically young gravitational systems still in formation. Numerical simulations clearly show that the mass distribu-

tion of clusters of galaxies, their radial mass profile as well as the evolution of cluster abundance with redshift strongly depend on cosmological models and can be used in order to measure the cosmological parameters, like Ω_m or σ_8 . Earlier work on cluster lensing revealed however that these systems are in general dynamically and thermodynamically complex and hard to interpret from their baryonic content only using simple models.

Because gravitational lensing analysis only probes matter regardless the complexity of its internal physical properties, it is an interesting alternative tool to standard virial and X-ray studies. From a weak lensing technical point of view, clusters of galaxies are well suited systems for mass reconstruction: their mass-density contrast is high enough (> 100) to produce significant gravitational distortion, and their angular scale (≥ 10 arc-minutes) is much larger than the typical angular distance between the lensed background galaxies. Therefore mass reconstruction in cluster of galaxies is quite easy and robust, and the angular resolution good enough for scientific purpose (about 1 arcmin).

The present status of weak lensing mass reconstruction of distant clusters of galaxies is listed in [10]. This sample only contains clusters with a redshift larger than 0.1 and does not include those analyzed with the magnification bias (or depletion) technique. Despite an important dispersion due to an heterogeneous sample, some general trends emerge. The averaged mass-to-light ratios from weak lensing (WL) is $(M/L)_{WL} \approx 400 h$ (with a dispersion of $\pm 200 h$) and the typical velocity dispersion is 1000 km/sec. Assuming that all the mass is contained in clusters, this corresponds to $\Omega_{m-WL} \approx 0.28$, which is in good agreement with X-ray or virial analyses as well as strong lensing studies based of giant arc reconstruction in clusters of galaxies.

Unfortunately, the differences between isothermal, power law or NFW “universal” models are still smaller than the errors of the measured mass profile (see for example [11]). The fact that giant arcs statistic is in favor of highly peak mass profile is not enough to distinguish between the different theoretical profiles. In fact, in view of the present signal-to-noise ratio of mass maps and the large family of analytical mass profiles which are proposed, this issue will demand important improvements in the shear measurement and to stack together many cluster profiles. It is important to notice that the difficulty to separate all the analytical mass profiles from weak lensing reconstruction is coming from random noise and not from intrinsic problems with mass reconstruction (which has been extensively studied and tested). This is well confirmed from the comparison between weak lensing and X-ray analyses: for instance, the recent comparison of lensing studies in Abell 2390 with Chandra observations ([12]) show a remarkable agreement of the mass profiles which confirm *a posteriori* that mass reconstruction are reliable.

In contrast to the rather good agreement observed between weak lensing and X-ray, frequent discrepancies are reported on small scales with strong lensing reconstructions. Part of the discrepancy is due to gravitational lensing and is likely a projection effect of matter located anywhere along the line of sight of clusters ([13], [14]). But on very small scale, inside the innermost regions, physical properties of clusters are complex and a simplistic description of hot baryons is no longer valid. [15] observed that the discrepancy is only significant in clusters without cooling flow of intra-cluster gas. Since cooling flows are only detected in the densest systems which are also the most dynamically evolved, the tendency he reported reveals that only young clusters show a discrepancy. If so, it is likely that their dynamics and thermodynamics models of these clusters are oversimplified.

4 Dark clusters

The unknown contribution to dark matter which could not be detected by any method but gravitational lensing would be the so-called “dark clusters”. The most convincing cases reported so far (HST/STIS field, Miralles et al 2001 - private communication; Abell 1942, [16]; Cl1604+4304, [17]; Cl0024+1654, [18]) show a clear shear pattern spread over angular scale of one arcminute. Their typical mass, estimated from reasonable assumptions on their redshift, is about $10^{14} M_\odot$ and corresponds to $M/L \gg 500$.

It is not clear yet whether dark clusters are real physically bound systems. An alternative view is that they are indeed very high redshift clusters: they are not detected because they are too faint and because most of its optical light is shifted toward the infrared. This possibility has been explored by [19] who carried out very deep H-band observations of Abell 1942. But nothing has been detected so far. It is also possible that these systems do not have bright galaxies but do have a hot intra-cluster gas. So far, none of them have been observed deeply in X-ray telescopes, so it is not demonstrated yet that dark clusters do not contain baryonic matter.

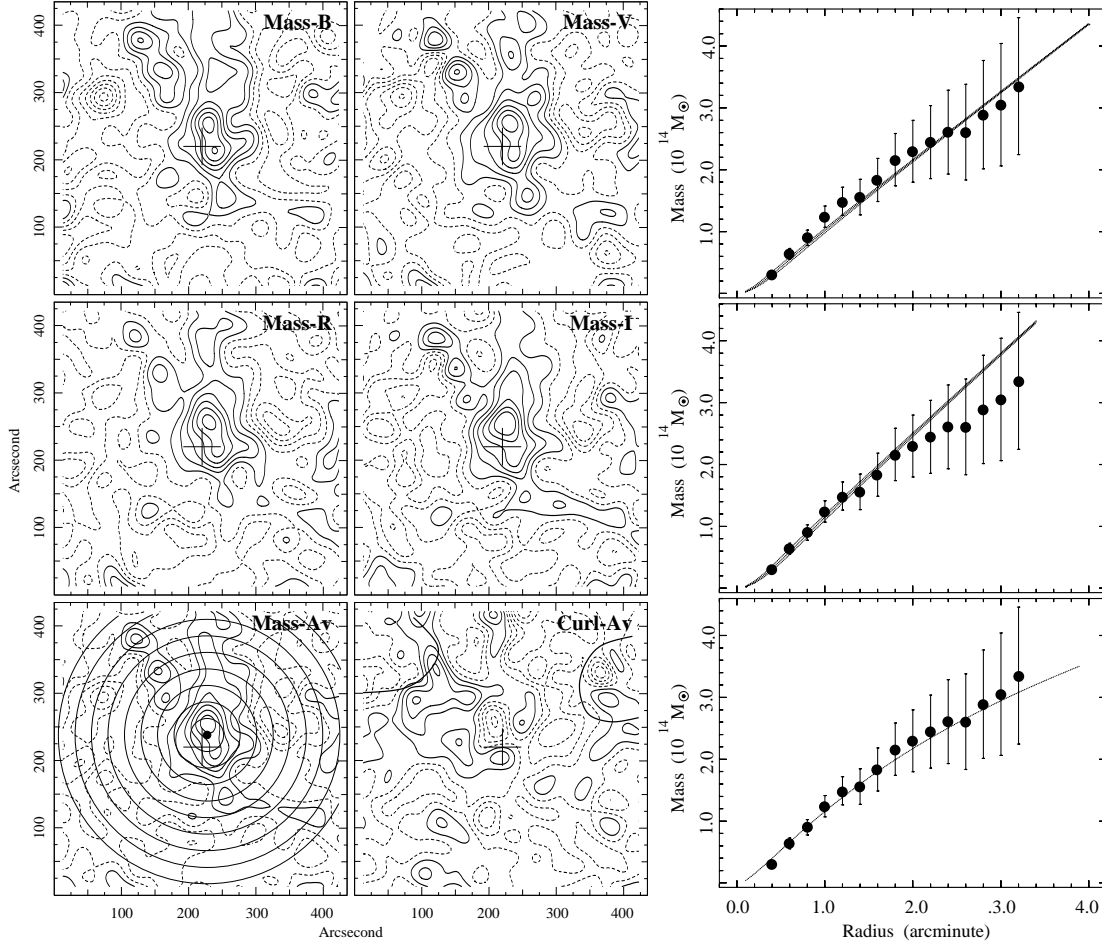


Figure 1: Mass reconstruction of the distant cluster MS1008 using weak lensing. The left panel show 4 mass reconstructions done independently using B,V, R and I data obtained at the VLT/UT1. The bottom left panel show the final reconstruction using the 4 filters jointly. The bottom right show random noise when galaxies are rotated by 90 degrees. On the right panel the radial mass profile is compared to an isothermal sphere with 950 km/sec (top), 1080 km.sec (middle) and the best NFW fit (bottom). Both top and bottom panel fit equally well the data (from [20]).

The key question is now to confirm that dark clusters exist or whether these detections are fortuitous fluctuations along some line of sights. “Dark clusters” could also be produced by intrinsic alignment, or just systematics. This is a difficult issue: up to now we have no way, but gravitational lensing, to “see” them, and if they contain neither galaxies nor hot gas, we cannot measure their redshift. From a cosmological point of view, the existence of such systems is a theoretical challenge. In particular, it seems difficult to produce a selective gravitational collapse which would accrete only non-baryonic dark matter without simultaneous baryonic collapse. From the point of view of dark matter and dark cluster abundance, if dark clusters include a large fraction of mass, then the mass fraction and the cluster abundance in the universe have been underestimated. Whether they contribute significantly to Ω_m has to be clarified. Assuming a flat universe with $\Omega_{\Lambda} \approx 0.7$, there is still enough uncertainty in Ω_m to allow dark clusters (DC) to contribute up to $\Omega_{m-DC} \approx 0.1$ without facing contradiction with what we learned from other mass estimates.

5 Cosmic shear

The light propagation through an inhomogeneous universe accumulates weak gravitational deflections over Gigaparsec distances. The theoretical works pioneered about 40 years ago initiated a long series of theoretical and observational analysis, which came to successful detections two years ago. The developments in this field went incredibly fast and revealed some of the interesting cosmological

applications of cosmic shear.

5.1 Gravitational deflection in inhomogeneous universe

Assuming structures formed from gravitational growth of Gaussian fluctuations, gravitational deflections on cosmological scales can be predicted from Perturbation Theory. To first order, the convergence $\kappa(\boldsymbol{\theta})$ at angular position $\boldsymbol{\theta}$ is given by the line-of-sight integral

$$\kappa(\boldsymbol{\theta}) = \frac{3}{2}\Omega_0 \int_0^{z_s} n(z_s) dz_s \int_0^{\chi(z)} \frac{D(z, z_s) D(z)}{D(z_s)} \delta(\chi, \boldsymbol{\theta}) [1 + z(\chi)] d\chi, \quad (5)$$

where $\chi(z)$ is the radial distance out to redshift z , D the angular diameter distances, $n(z_s)$ is the redshift distribution of the sources and δ the mass density contrast responsible for the deflection at redshift z . δ depends on the properties of the power spectrum and tells us how the gravitational convergence field depends on the cosmic history of structure formation. Similarly, the cumulative weak lensing effects of structures also induce a shear field correlated with the projected mass density which can be characterized by the 2-point shear (*ie* ellipticity) correlation function:

$$\langle \gamma\gamma \rangle_\theta = \frac{1}{2\pi} \int_0^\infty P_\kappa(k) J_0(k\theta) dk, \quad (6)$$

where $P_\kappa(k)$ is the power spectrum of the convergence field. Note that to first order we have $\langle \gamma\gamma \rangle_\theta = \langle \kappa\kappa \rangle_\theta$. A measurement of this correlation function and of the skewness of the convergence, $s_3(\theta)$, which probes non Gaussian features in the projected mass density field, describe most of cosmological properties of the convergence field (see [21]; [22] and references therein). This is easy to demonstrate with a simple calculation based on perturbation theory and assuming a power law mass power spectrum. Assuming no cosmological constant, and a background population at a single redshift z , $\langle \kappa(\theta)^2 \rangle$ and $s_3(\theta)$ can be analytically calculated:

$$\langle \kappa(\theta)^2 \rangle^{1/2} = \langle \gamma(\theta)^2 \rangle^{1/2} \approx 1\% \sigma_8 \Omega_m^{0.75} z_s^{0.8} \left(\frac{\theta}{1 \text{ arcmin}} \right)^{-\left(\frac{n+2}{2}\right)}, \text{ and} \quad (7)$$

$$s_3(\theta) = \frac{\langle \kappa^3 \rangle}{\langle \kappa^2 \rangle^2} \approx 40 \Omega_m^{-0.8} z_s^{-1.35}, \quad (8)$$

where n is the spectral index of the power spectrum of density fluctuations. It shows that in principle the degeneracy between Ω_m and σ_8 is broken when both the variance and the skewness of the convergence are measured. Note that the true relationship between all the cosmological parameters and the measurement for realistic models (that is including CDM power spectrum, broad redshift distribution and non-linear effects) is in fact more complicated, but these equations faithfully reflect the main dependencies.

5.2 Expectations

From an observational point of view, cosmic shear surveys turn out to be a difficult task. [23] clarified the strategy by exploring the properties of the variance and the skewness of the convergence for various cosmological scenarios. They conclude that the variance can provide cosmological information, provided the survey size is about 1 deg^2 , whereas for the skewness at least 10 deg^2 must be covered and more than 100 deg^2 for information on Ω_Λ or the shape of the power spectrum over scales larger than 1 degree.

Like in the precedent Section, assuming perturbation theory and a power law power spectrum with $n = 1$, we can derive the shear variance as a function of the survey characteristics. For example for $\Omega_m = 0.3$ and $\sigma_8 = 1$, we have:

$$\langle \gamma(\theta)^2 \rangle^{1/2} = 0.3\% \left[\frac{A_T}{100 \text{ deg}^2} \right]^{\frac{1}{4}} \times \left[\frac{\sigma_{\epsilon_{gal}}}{0.4} \right] \times \left[\frac{n}{20 \text{ arcmin}^{-2}} \right]^{-\frac{1}{2}} \times \left[\frac{\theta}{10'} \right]^{-\frac{1}{2}}, \quad (9)$$

where A_T is the total sky coverage of the survey. The numbers given in the brackets correspond to a measurement at $3 - \sigma$ confidence level of the shear variance. However, technical issues regarding

Table 1: Present status of cosmic shear surveys with published results.

Telescope	Pointings	Total Area	Lim. Mag.	Ref..
CFHT	$5 \times 30' \times 30'$	1.7 deg^2	I=24.	[25][vWM E+]
CTIO	$3 \times 40' \times 40'$	1.5 deg^2	R=26.	[26][WTK +]
WHT	$14 \times 8' \times 15'$	0.5 deg^2	R=24.	[27][BRE]
CFHT	$6 \times 30' \times 30'$	1.0 deg^2	I=24.	[28][KWL]
VLT/UT1	$50 \times 7' \times 7'$	0.6 deg^2	I=24.	[29][Mv WM+]
HST/WFPC2	$1 \times 4' \times 42'$	0.05 deg^2	I=27.	[30]
CFHT	$4 \times 120' \times 120'$	6.5 deg^2	I=24.	[31][vW MR+]
HST/STIS	$121 \times 1' \times 1'$	0.05 deg^2	$V \approx 26$	[32]
CFHT	$10 \times 126' \times 140'$	$16. \text{ deg}^2$	R=23.5	[33]
CFHT	$4 \times 120' \times 120'$	8.5 deg^2	I=24.	[34]

corrections of atmospheric and optical distortions are the major concerns and the main limitations. The present-day systematic residuals prevent us to measure gravitational shear amplitude smaller than 0.3-0.5% ([24]). Translated into angular scale, it means that we are presently limited to $\theta \approx 2^\circ$, that is where the expected signal equals the residual systematics.

5.3 Observational results

Table 1 lists cosmic shear surveys with already published results. This is not an exhaustive summary because many surveys are still going on at SUBARU, CTIO, NOAO, CFHT, HST or WHT and several are also planned within the next decade with new facilities. The different strategies adopted by each group enables to handle carefully and in different manner all sources of noise as well as systematics. It is indeed important to keep a variety of approaches in order to cross-check results and consistency of cosmological interpretations and, in the future to use all these samples together.

From these surveys, it has been possible to recover the amplitude of the cosmic shear variance as function of angular scale. Figure 2 show the remarkable agreement between surveys¹. This plot is the most convincing result showing the existence of a correlation of ellipticities of galaxies in the universe. It is indeed interpreted as a cosmological weak lensing effect of large-scale structures of the universe. However, we should keep in mind that a robust and definitive cosmological interpretation of these measurements remain dependent on our ability to pin down the residual systematics and/or to separate signal and systematics as the E-B mode decomposition seems to be able to make it ([34]). Another important aspect is the necessity to improve our knowledge of the redshift distribution, which seems possible with the photometric redshift technique.

5.4 Cosmological outcomes

Comparison with some realistic cosmological models are plotted in Figure 2. The amplitude of the shear has been scaled assuming that sources are at $\langle z \rangle \approx 1$, as expected from the comparison of the photometric depth of these surveys with the deepest spectroscopic surveys done so far. The standard COBE-normalized CDM is ruled at a 10- σ confidence level. However, there are many models which fit the data. This simply illustrates the degeneracy between Ω_m and σ_8 we discussed in the previous section and which cannot be broken without high-order statistics. A plot with Ω_m - σ_8 confidence level contours is more meaningful, as in Fig. 3. The left and middle panels show two independent data sets, both containing almost the same number of galaxies. The left panel is a compilation of the five first survey of the previous figure. It covers 6.5 deg^2 over 75 independent areas and contains 250,000 galaxies. The middle panel is the CFH-2 survey (see figure 2) which covers 8.5 deg^2 over 4 independent fields and contains 450,000 galaxies. Both Ω_m - σ_8 contours are difficult to reconcile observations with an $\Omega_m > 0.8$ -universe. Assuming a CDM model with $\Gamma \approx 0.2$, we can conclude that reasonable cosmological models have:

$$0.05 \leq \Omega_m \leq 0.8 \quad \text{and} \quad 0.5 \leq \sigma_8 \leq 1.2 . \quad (10)$$

¹ [33] data are missing because depth is different so the sources are at lower redshift and the amplitude of the shear is not directly comparable to other data plotted

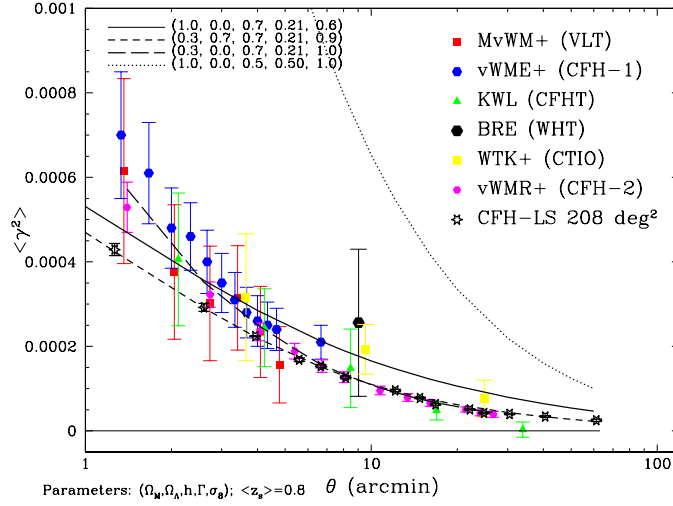


Figure 2: Top hat variance of shear as function of angular scale from 6 cosmic shear surveys. The CFH-LS (open black stars) illustrates the expected signal from a large survey covering 200 deg². For most points the errors are smaller than the stars.

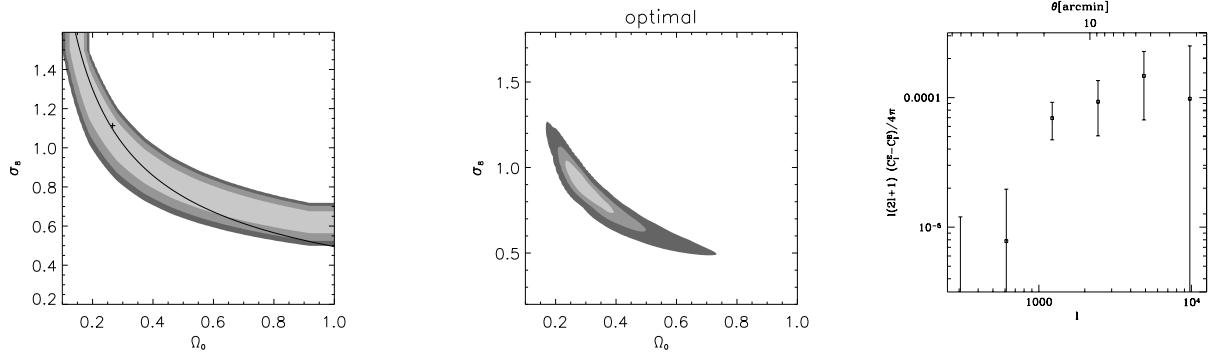


Figure 3: Cosmological results from cosmic shear surveys: the two left-hand panel are $\Omega_m - \sigma_8$ cl contour plots from two independent data sets. The left panel is a compilation of five surveys (from Maoli et al. 2001). The central panel only comes from van Waerbeke et al. (2001). On the right, the angular power spectrum of the convergence field from the VIRMOS-DESCART survey is plotted (From Pen et al 2001).

A more detailed investigation of the data also permits to probe the power spectrum of the dark matter on scale below 30 arc-minutes. [34] cleaned first the CFH-2 sample of the VIRMOS-DESCART cosmic shear survey² from systematics residuals. This is possible by separating the shear field into curl-free and curl modes (called E and B modes respectively). This is identical to the technique expected to take place on the cosmic microwave background polarization analysis. In the case of weak lensing, the residual are expected to contribute equally to the E and B modes, while the cosmic shear signal shows up only in the E channel. By separating the E - and B - components of the shear field, [34] succeeded to reduce errors by a factor of $\sqrt{2}$ of the pure gravitational lensing signal. Then, they computed each $C(l)$ from the E -mode in a standard way. They are shown on Figure 3. Since they are inferred from weak distortion of galaxies only, they represent a direct measurement the projected dark matter power spectrum. The data cover a small area, are still confined inside the range $1' \leq \theta \leq 30'$ ($5 \times 10^2 \leq l \leq 10^4$) and are noisy. However, the signal is strong enough to be compared with cosmological models or other $C(l)$ inferred from redshift surveys or the CMB. It shows the potential of future cosmic shear surveys, in particular that it will be possible to measure the 3D mass power spectrum with accurate measurements.

²<http://terapix.iap.fr/Descart> and <http://www.astrsp-mrs.fr/virmos/>

5.5 Systematics and calibration issues

There are four major concerns regarding the amplitude and the interpretation of the weak distortion signal. (1) systematics produced by wrong or insufficient PSF anisotropy correction; (2) systematics produced by real but non-lensing signal producing similar distortion as cosmic shear, like intrinsic correlations of ellipticities (3) wrong scaling of redshift distribution of sources, and (4) source clustering.

All of them have been analyzed at length. Careful tests regarding PSF anisotropy corrections demonstrate that residuals are small on scale ranging from 1 arc-minute to 30 arc-minutes. The intrinsic correlations of ellipticities which could be generated during galaxy formation processes may produce similar signatures as cosmic shear. Several recent numerical and theoretical studies (see for example [35]; [36]) show that intrinsic correlations are negligible on scales beyond one arc-minute, provided that the survey is deep enough. In that case, most lensed galaxies along a line of sight are spread over Gigaparsec scales and have no physical relation with its apparent neighbors. Since most cosmic survey are deep, they are almost free of intrinsic correlations. [34], in particular, have confirmed that the VIRMOS-DESCART survey listed in Table 1 shows a pure cosmic shear signal on scales beyond one arc-minute, which dominates any systematics by significant factor. In contrast, shallow surveys may have strong contamination. Although it weakens the interest of shallow survey for cosmic shear, they are nevertheless interesting since it give us insight on properties of intrinsic ellipticity correlations produced by the generation of angular momentum during merging processes of halos.

Likewise redshift of arcs which scale the total mass inside a critical radius, the redshift of sources used for cosmic shear analysis scales the amplitude of the shear. Current surveys probe sources up to $I \approx 24$. This is within the limits of giant telescopes, so detailed informations on redshift distributions of lensed galaxies will be soon well constrained³. Beyond this limit, there is no possibility to get spectroscopic redshifts of sources and only photometric redshifts are expected to work. Present-day calibrations show that the technique works well enough to provide source redshift with sufficient accuracy up to $I \approx 25$. Beyond this, it may be more critical.

The difficulties may be with clustering of sources which seems to significantly affect high-order statistics, like skewness ([37]). Uncertainties on the amplitude of the skewness produced by clustering may be as high as 30% . If so, multi-lens plane cosmic shear analysis will be necessary which implies a good knowledge of the redshift distribution. For very deep cosmic shear surveys, this could be could be a challenging issue.

6 Conclusions and prospects

Tracing the matter and its evolution with look-back time is a major goal of all massive surveys done with ground based telescopes or satellites. Weak gravitational lensing is a new but reliable tool for this purpose because it is almost insensitive on the nature and the physical stage of the matter. Past and present experiences show that it can provide astrophysical informations at about all scales ranging from 10 kpc to 1 Gpc and address as well key scientific question relevant for fundamental physics.

In this review we focussed on galaxies, cluster of galaxies and large-scale structures. But first tentatives by Hoekstra et al ([38]) on the CNOC2 surveys on groups of galaxies and by Kaiser et al 1998 ([39]) on a supercluster of galaxies will be soon widely deployed on very large samples in order to understand the physics of these systems and their interactions with galaxy halos, clusters and very large structures. Used jointly with cosmic shear analysis, we expect that these surveys will provide a complete description of the dark matter, with particular emphasis on the properties of its power spectrum, the radial mass profile of bound systems and the coupling between baryonic and non-baryonic matter. This last point is now underway. The recent analysis on the biasing and galaxy-mass cross correlation coefficient in the RCS survey by Hoekstra et al show that we can now test whether the linear biasing is valid and probe the relation between mass and light as function of angular scale ([40]; [41]). Similar studies can be done inside clusters of galaxies by using jointly weak lensing, X-ray and SZ reconstructions ([42], [43]).

Next cosmic shear survey generation with MEGACAM at CFHT or VST/VISTA at Paranal or even space based panoramic cameras will improve by one order of magnitude in details and precision (see figure 2). It is expected that they will provide accurate projected mass reconstruction, similar to APM

³Using the DEEP2 ([44] Davis et al. 2000) or VIRMOS ([45] Le Fèvre et al. 2000) surveys for example.

galaxy survey. They should be able to break the degeneracy between Ω_m and σ_8 from the analysis of the skewness of κ . On a longer time-scale, very large cosmic shear surveys will probe the dark matter power spectrum over scales larger than 10 degrees and will permit to constrain Ω_Λ , or any quintessence fields ([46]; [47]).

Acknowledgements

We thank R. Athreya, K. Benabed, F. Bernardeau, E. Bertin, O. Doré, B. Fort, H. Hoekstra, B. Jain, P. Schneider, for useful discussions. This work was supported by the TMR Network “Gravitational Lensing: New Constraints on Cosmology and the Distribution of Dark Matter” of the EC under contract No. ERBFMRX-CT97-0172. YM thanks the organizers of the meeting for financial support.

References

- [1] Mellier, Y.; 1999 ARAA 37, 127.
- [2] Bartelmann, M.; Schneider, P.; 2001 Phys. Rep. 340, 292.
- [3] Brainerd, T.G., Blandford, R.D., Smail, I. 1996 ApJ466, 623.
- [4] Schneider, P.; Rix, H.-W. 1997 A&A 474, 25.
- [5] Tyson, A.J.; Valdes, F.; Jarvis, J.F.; Mills, A.P. 1984 ApJ281, L59.
- [6] McKay, T. et al. 2001 preprint, astro-ph/0108103.
- [7] Smith, D.R.; Bernstein, G.M.; Fischer, P.; Jarvis, M. 2000 Preprint astro-ph/0010071
- [8] Wilson, G., Kaiser, N., Luppino, G.A.; 2001 ApJ556, 601.
- [9] Keeton, C.R. 2001, preprint, astro-ph/0105200.
- [10] Mellier, Y.; 2001 Proceedings of the the ISSI workshop “Matter in the Universe”, Vol. 15. Ph. Jetzer, K. Pretzl and R. von Steiger Eds. Kluwer Academic Press.
- [11] Clowe, D.; Luppino, G.; Kaiser N.; Gioia, I.M.; 2000 ApJ 539, 540.
- [12] Allen, S.W., Ettori, S.; Fabian, A.C. 2001 MNRAS 324, 877.
- [13] Reblinsky, C.; Bartelmann, M; 1999 A&A345, 1.
- [14] Metzler, C.; White, M.; Michael, N.; Loken; 1999 AJ520, L9.
- [15] Allen, S.W.; 1998 MNRAS 296, 392.
- [16] Erben, T.; van Waerbeke, L.; Mellier, Y.; et al. 2000 A&A 355, 23.
- [17] Umetsu, K.; Futamase, T.; 2000 ApJ 539, 5.
- [18] Bonnet, H.; Mellier, Y.; Fort, B. 1994 ApJ427, L83.
- [19] Gray, M.; Ellis, R.S.; Lewis, J.R.; McMahon, R.G.; Firth, A.E.; 2001 MNRAS 325, 111.
- [20] Athreya, R.; Mellier, Y.; van Waerbeke, L.; et al. 1999 preprint, astro-ph/9909518.
- [21] Bernardeau, F.; van Waerbeke, L.; Mellier, Y.; 1997 A&A 322, 1.
- [22] Jain, B.; Seljak, U.; 1997 ApJ 484, 560.
- [23] van Waerbeke, L.; Bernardeau, F.; Mellier, Y.; 1999 A&A 342, 15.
- [24] Erben, T.; van Waerbeke, L.; Bertin, E.; Mellier, Y.; Schneider, P.; 2001 A&A 366, 717.

- [25] van Waerbeke, L.; Mellier, Y.; Erben, T.; et al.; 2000 A&A 358, 30 [vWME+].
- [26] Wittman, D.; Tyson, J.A.; Kirkman, D.; Dell’Antonio, I.; Bernstein, G. 2000a Nature 405, 143 [WTK+].
- [27] Bacon, D.; Réfrégier, A., Ellis, R.S.; 2000 MNRAS 318, 625 [BRE].
- [28] Kaiser, N., Wilson, G., Luppino, G. 2000 preprint, astro-ph/0003338 [KWL].
- [29] Maoli, R.; van Waerbeke, L.; Mellier, Y.; et al.; 2001 A&A 368, 766 [MvWM+].
- [30] Rhodes, J.; Réfrégier, A., Groth, E.J.; 2001 ApJ 536, 79.
- [31] van Waerbeke, L.; Mellier, Y.; Radovich, M.; et al.; 2001 A&A 374, 757 [vWMR+].
- [32] Hämmerle, H.; Miralles, J.-M.; Schneider, P.; Erben, T.; Fosbury, R.A.E.; Freudling, W.; Pirzkal; N., Jain, B.; White, S.D.M.; 2001 Submitted
- [33] Hoekstra, H.; Yee, H., Gladders, M.D. 2001 ApJ 558, L11
- [34] Pen, U.; van Waerbeke, L.; Mellier, Y.; 2001 preprint, astro-ph/0109182.
- [35] Crittenden, R.G.; Natarajan, P.; Pen, U.; Theuns, T. 2000 preprint astro-ph/0012336.
- [36] Mackey, J.; White, M.; Kamionkowski, M.; 2001 preprint, astro-ph/0106364.
- [37] Hamana, T. et al. 2000. preprint astro-ph/0012200
- [38] Hoekstra, H.; et al. 2001 ApJ 548, 5
- [39] Kaiser, N., Wilson, G., Luppino, G.; Kofman, L.; Gioia, I.; Metzger, M.; Dahle, H. 1998 preprint, astro-ph/9809268.
- [40] Schneider, P.; 1998 A&A 498, 43.
- [41] van Waerbeke, L.; 1998 A&A 334, 1.
- [42] Zaroubi, S.; Squires, G.; Hoffman, Y.; Silk, J.; 1997 ApJ 500, 87.
- [43] Doré, O., Bouchet, F., Mellier, Y., Teyssier, R.; 2001 A&A 375, 14.
- [44] Davis, M.; Newman, J.; Faber, S.; Phillips, A.; 2000 Proc. ESO/ECF/ESA on Deep Fields Springer.
- [45] Le Fèvre, O.; Saisse, M.; Mancini, M.; 2000 SPIE 4008, 546.
- [46] Hu, W.; Tegmark, M. ApJ 514, 65.
- [47] Benabed, K.; Bernardeau, F.; 2001 preprint, astro-ph/0104371.